

the line<sup>19,20</sup>

$$g(\nu) = 2\tau/[1 + 4\pi^2\tau^2(\nu - \nu_0)^2]. \quad (1)$$

Here  $\tau$  is the average lifetime of the vacancy in the position giving rise to the resonance line being observed, where only jumps which change the spectrum are considered as contributing to  $\tau$ .<sup>21</sup>

If we observe a resonance line at frequency  $\nu_i$  which is produced by a vacancy in the  $i$ th site, the requirement for losing phase coherence during the time the vacancy is away can be estimated as follows: The average time spent at site  $j$  before the vacancy returns can be determined by simple detailed balance arguments and is given by  $\tau_i p_j / p_i$ . Here  $\tau_i$  is the average lifetime in the  $i$ th site and  $p_j$  and  $p_i$  are the probabilities

of finding the vacancy in the  $j$ th and  $i$ th site, respectively. The average phase error accumulated at site  $j$  is therefore  $2\pi\tau_i(\nu_j - \nu_i)p_j/p_i$ . In order that phase coherence be lost, the total average phase error accumulated before the vacancy returns to site  $i$  must be  $\gtrsim 2\pi$ . Summing over all sites  $j$ , this gives the requirement

$$(\tau_i/p_i) \sum_j p_j(\nu_j - \nu_i) \gtrsim 1. \quad (8)$$

Only nearest and next nearest vacancy- $Mn^{++}$  pairs are observed. Thus the  $p_j$  are small for other vacancy sites and only the motion between the nearest and next nearest sites need be considered. With the values of  $\nu_j$  and  $p_j$  determined from the resonance (see A), Eq. (8) gives  $\tau \gtrsim 1.5 \times 10^{-10}$  sec for the nearest neighbor multiplet and  $\tau \gtrsim 6 \times 10^{-10}$  sec for the next nearest. At the highest temperature studied the deduced lifetimes are still a factor of ten larger than these limits. We therefore conclude that Eq. (1) is valid over the range of temperatures studied and  $\tau$  gives the lifetime of the vacancy site giving rise to the multiplet studied.

<sup>19</sup> M. C. Wang and G. E. Uhlenbeck, *Revs. Modern Phys.* **17**, 326 (1945).

<sup>20</sup> I. Yokota, *Progr. Theoret. Phys. (Japan)* **8**, 380 (1952).

<sup>21</sup> We assume that the time required for the jump is very short compared to the time between jumps. As a result possible phase accumulation during the jump is not considered.

## Configuration Coordinate Model for KCl:Tl Including Spin-Orbit Interaction

F. E. WILLIAMS AND P. D. JOHNSON

*General Electric Research Laboratory, Schenectady, New York*

(Received September 2, 1958)

The effect of the crystalline field on the spin-orbit interaction of the  $^3P^0$  and  $^1P^0$  states of  $Tl^+$  in KCl has now been included in the configuration coordinate model. The potential energy curves for the pure spin states are required to satisfy the condition that after the application of spin-orbit interaction the resulting crystal states account for the absorption and emission spectra, explained by the earlier model, and for the oscillator strengths of the absorption bands. In accordance with the adiabatic approximation, the potential energy curves for the states involved in absorption and emission do not cross and the electronic matrix elements for radiative transitions depend on the configuration coordinate. The curve for the lower excited state has two minima which account for the 3050 Å and the 4750 Å emission bands. From the single minimum of the upper excited state an additional emission band near the 2470 Å absorption band is predicted. With intense excitation at 77°K in a narrow spectral range near 1960 Å, which corresponds to excitation only to the upper excited state, the predicted emission has been found. The existence and characteristics of the new emission provide confirmation of the model, particularly of the quantitative effect of spin-orbit interaction.

### I. INTRODUCTION

THE configuration coordinate model has been used extensively to explain the properties of localized impurity systems in luminescent crystals. This model is based on the adiabatic approximation according to which the wave function  $\psi(r, q)$  for a state of the impurity system can be written

$$\psi(r, q) = \phi(q) \varphi(r, q). \quad (1)$$

The electronic wave function  $\varphi(r, q)$  is a function of the electronic coordinates  $r$  and is smoothly modified by changes in the positions,  $q$ , of the nuclei whose state of motion is described by  $\phi(q)$ . In other words, transitions between electronic states do not occur during the changes in nuclear coordinates but rather an electronic

state itself is progressively deformed during an adiabatic change in nuclear coordinates. In this approximation an effective potential, therefore, exists for nuclear displacements and it can be shown that this potential may contain terms up to the fourth power of the displacements.<sup>1</sup>

The configuration coordinate model involves a diagrammatic representation of the energy of the system as a function of adiabatic displacements in the nuclear coordinates. The energy is plotted as a function of the nuclear coordinates of the crystal for each electronic state of the system. Optical transitions occur vertically in accordance with the Frank-Condon principle. In the

<sup>1</sup> M. Born and K. Huang, *Dynamic Theory of Crystal Lattices* (Oxford University Press, Oxford, 1954), p. 171.

early interpretations of luminescence in solids, based on this model, the single configuration coordinate used was regarded as schematic for the  $3N$  real coordinates involved, where  $N$  is the number of atoms comprising the luminescent center. The model qualitatively accounted for the Stokes shift of emission compared to excitation spectra, the width of these bands, and the phenomenon of thermal quenching of luminescence.<sup>2,3</sup> The representation of a many-coordinate impurity system by a single-coordinate model has been justified by quite general arguments.<sup>4</sup>

A configuration coordinate model involving a single real coordinate has been used for thallium-activated potassium chloride.<sup>5</sup> The symmetric radial displacement of the six chloride ions which are nearest neighbors to the thallous ion was used as the configuration coordinate, and the energy of this impurity system was calculated by modified Born-Mayer methods for the ground  $^1S$  state with the  $6s^2$  configuration and for the excited  $^3P_1^0$  state with the  $6s6p$  configuration of  $Tl^+$ . In this calculation the harmonic approximation<sup>1</sup> was used, that is, the dependence of the electronic wave function  $\varphi(r, q)$ , and consequently the dependence of the dipole matrix element, on the nuclear coordinates  $q$  was neglected. The theoretical results accounted semiquantitatively for the long wavelength absorption and associated emission spectra,<sup>5</sup> and for their temperature<sup>6</sup> and pressure dependence.<sup>7</sup> Subsequently, the configuration coordinate model for  $KCl:Tl$  was modified and extended to other excited states by determining the energy contours empirically so as to be consistent with the experimental data.<sup>8-10</sup> The higher excited state responsible for the additional absorption and emission bands was found to have the characteristics expected theoretically for the  $^1P_1^0$  state of  $Tl^+$  with the  $6s6p$  configuration. In addition, trapping states were tentatively identified. This work has resulted in a simple model which is in quantitative accord with the absorption and emission bands and with the kinetic processes accompanying luminescence in  $KCl:Tl$ . The effect of the crystalline field on the spin-orbit interaction of the  $^1P^0$  and  $^3P^0$  state was not included in these investigations. In fact, the contours for the  $^1P_1^0$  and  $^3P_1^0$  states were allowed to cross in violation of a requirement for the adiabatic approximation. The requirement is that the separation of the electronic states  $\Delta E$  at fixed  $q$  be related to the frequency of lattice vibrations

$\nu_N$  as follows:

$$\Delta E \gg h\nu_N. \quad (2)$$

However, since the electronic transitions occur at configurations sufficiently removed from the crossing for Eq. (2) to apply, the model just described is valid for explaining absorption and emission spectra known at that time.

Recently, in an analysis of the relative oscillator strengths of the impurity absorption bands in  $KCl:Tl$  and  $KCl:In$ ,<sup>11</sup> crystalline interactions were found to decrease the energy separation  $2G$  of the pure  $^1P^0$  and  $^3P^0$  spin states for the equilibrium configuration of the  $^1S$  ground state. This change in the energy separation  $2G$  alters the ratio of oscillator strengths for the transitions from the  $^1S$  ground state to the  $^1P_1^0$  and  $^3P_1^0$  crystal states compared to the corresponding transitions of the free ions. Because crystalline interactions alter the energy separation  $2G$  over the entire range of nuclear coordinates involved in the luminescence, we have now re-examined the configuration coordinate model for  $KCl:Tl$  taking into account the dependence of the mixing of the pure spin states on the nuclear coordinates. In this way, the potential energy contours are modified, a new emission band is predicted, and the model now satisfies the condition for the adiabatic approximation given by Eq. (2).

## II. DERIVATION OF THE CONFIGURATION COORDINATE DIAGRAM

The configuration coordinate  $q$  is taken to be the symmetrical displacement radially from the  $Tl^+$  of the six nearest-neighbor  $Cl^-$  from their perfect lattice sites. It has been shown that the transition energy  $\Delta E$  between states is most strongly dependent on this coordinate.<sup>5</sup> The remainder of the ions of the crystal are allowed to relax to positions minimizing the crystal energy for each value of the nearest-neighbor displacement. The configuration coordinate curves are, therefore, asymmetric for large displacements. A greater stiffness is encountered on displacing the nearest-neighbors toward, compared to away from, the  $Tl^+$ . This asymmetry, however, was not evident in the original theoretical calculations,<sup>5</sup> the curves being parabolic. In the present model it was found necessary to include the asymmetry for the excited pure spin states by means of a cubic term in order to fit all the available experimental data. The parabolic term, of course, remains a satisfactory approximation for small displacements.

Since spin-orbit interaction does not affect the  $^1S$  ground state and since the Born-Mayer methods are most accurate for the ground state, the configuration coordinate for this state is taken from the original calculation<sup>5</sup> of the detailed crystalline interactions. This curve is parabolic and is shown as the lowest curve in Fig. 1.

<sup>11</sup> Williams, Segall, and Johnson, *Phys. Rev.* **108**, 46 (1957).

<sup>2</sup> R. W. Gurney and N. F. Mott, *Trans. Faraday Soc.* **35**, 69 (1939).

<sup>3</sup> F. Seitz, *J. Chem. Phys.* **6**, 150 (1938); *Trans. Faraday Soc.* **35**, 79 (1939).

<sup>4</sup> M. Lax, *J. Chem. Phys.* **20**, 1752 (1952).

<sup>5</sup> F. E. Williams, *J. Chem. Phys.* **19**, 457 (1951).

<sup>6</sup> F. E. Williams and M. H. Hebb, *Phys. Rev.* **84**, 1181 (1951).

<sup>7</sup> P. D. Johnson and F. E. Williams, *Phys. Rev.* **95**, 69 (1954).

<sup>8</sup> P. D. Johnson and F. E. Williams, *J. Chem. Phys.* **20**, 124 (1952).

<sup>9</sup> P. D. Johnson and F. E. Williams, *J. Chem. Phys.* **21**, 125 (1953).

<sup>10</sup> P. D. Johnson, *J. Chem. Phys.* **22**, 1143 (1954).

TABLE I. Values of the parameters describing the energy of each of the pure spin states as a function of the configurate coordinate.

State	$q_0, \text{\AA}$	$E_0, \text{eV}$	$\alpha, \text{eV/\AA}^2$	$\beta, \text{eV/\AA}^3$
$^1S$	0.095	0.16	8.4	0
$^3P^\circ$	-0.06	5.61	9.0	-8.0
$^1P^\circ$	-0.48	4.88	9.0	-8.0

For the excited states we first construct configuration coordinate curves for the pure spin states such as the dashed curves in Fig. 1. In principle, these curves could be determined by solving the Hartree-Fock equations for the  $^1P^\circ$  and  $^3P^\circ$  impurity crystal states. A more feasible theoretical investigation would involve including the crystalline interactions after calculating the free-ion Hartree-Fock wave functions. In the present investigation, however, we determine the energy curves for the pure spin states by trial and error in such a way that after introducing spin-orbit interaction, agreement with the experimental properties was attained. The curves for the pure spin states, in addition to describing the effect of crystalline interactions on these states as a function of the configurations coordinate  $q$ , define the dependence of  $2G$  on  $q$ . The equations for the pure spin states shown in Fig. 1 are of the following form:

$$E = \alpha(q - q_0)^2 + \beta(q - q_0)^3 + E_0. \quad (3)$$

The parameters,  $q_0$ ,  $E_0$ ,  $\alpha$ , and  $\beta$  are given in Table I for the  $^1S$ ,  $^3P^\circ$  and  $^1P^\circ$  pure spin states.

With spin-orbit interaction, the energies of the two excited states  $E_\pm(q)$  at a particular configuration  $q$  are

$$E_\pm(q) = -\frac{1}{4}\zeta \pm \left\{ \left[ G(q) + \frac{1}{4}\zeta \right]^2 + \frac{1}{2}\lambda^2\zeta^2 \right\}^{1/2}, \quad (4)$$

where the zero of energy is taken as the average energy of the pure spin states at  $q$ , and  $\zeta$  and  $\lambda$  are the spin-orbit coupling parameters defined as follows:

$$\begin{aligned} \zeta &= \frac{e\hbar^2}{2m^2c^2} \int R_3 \left( \frac{1}{r} \frac{\partial V}{\partial r} \right) R_3 r^2 dr, \\ \lambda\zeta &= \frac{e\hbar^2}{2m^2c^2} \int R_1 \left( \frac{1}{r} \frac{\partial V}{\partial r} \right) R_3 r^2 dr, \end{aligned} \quad (5)$$

where  $R_1$  and  $R_3$  are the radial wave functions for the  $^1P^\circ$  and  $^3P^\circ$  states, respectively, and  $V$  is the potential. Since the largest contribution to Eq. (5) comes from regions inside the ion core and since in these regions the wave functions and potential are well approximated by the free-ion functions, it follows that  $\zeta$  and  $\lambda$  can be approximated reasonably by their free-ion values of 1.02 eV and 0.87, respectively.<sup>11</sup> The maximum in the function  $d\zeta/dr$  lies at  $1/200 \text{ \AA}$  and essentially all contributions to  $\zeta$  lie within a radius of  $1/20 \text{ \AA}$ . The energies of the excited states with total angular momentum  $J=1$  are shown by the solid curves in Fig. 1.

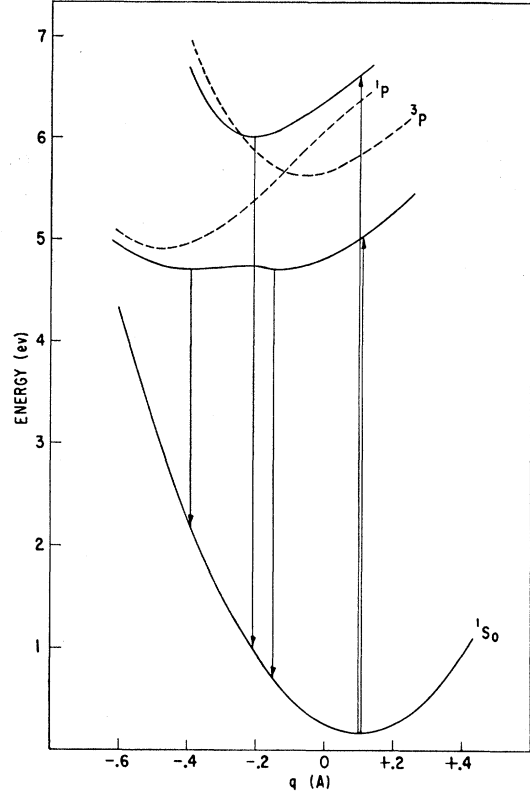


Fig. 1. Energy-configuration coordinate diagram for KCl:TI including spin-orbit interaction.

The number of adjustable parameters involved in the analysis was reduced by taking the coefficients  $\alpha$  and  $\beta$  to be the same for the  $^1P^\circ$  and  $^3P^\circ$  spin states. These coefficients plus the constants  $q_0$  and  $E_0$  for each of the spin states constitute six parameters. Because approximately twice this number of experimental data are consistent with Fig. 1, the model would appear to have appreciable fundamental significance. These data include the peak position of the two absorption and two emission bands, their half-widths, the dependence of the half-widths on temperature, the ratio of oscillator strengths of the absorption bands, the effect of hydrostatic pressure on the absorption spectrum, and the energy differences governing the occupational probabilities of the emitting states.

Configuration coordinate curves can also be obtained for the metastable  $^3P_0^\circ$  and  $^3P_2^\circ$  states of  $\text{TI}^+$ . In the approximation that the crystalline interactions are independent of  $J$  value, the  $^3P_0^\circ$  and  $^3P_2^\circ$  states are parallel to and displaced in energy  $-\zeta$  and  $+\frac{1}{2}\zeta$  from the  $^3P^\circ$  pure spin state. These states are believed to be responsible for some of the trapping phenomena observed<sup>9</sup> in KCl:TI and will not be considered further in this paper.

### III. CHARACTERISTICS OF THE MODEL

From Fig. 1 it is apparent that the curves which include spin-orbit interaction possess the important features of the earlier configuration coordinate diagrams<sup>5,8,10</sup> which are required to explain the experimental spectra. Including the dependence of the dipole matrix element on the configuration coordinate  $q$ , the spectrum  $Q_{\pm}(\Delta E)$  of an absorption or emission band involving the upper  $+$  or lower  $-$  excited state is of the following form:

$$Q_{\pm}(\Delta E) = C \left\{ \exp \left[ - (E - E_0) / k\theta \coth \frac{\theta}{T} \right] \left[ \frac{dq}{d\Delta E} \right] \right\} \times \left\{ \frac{[\frac{1}{2}\lambda^2\zeta^2 + (E_{\mp} - G)^2]\Delta E}{[\lambda^2\zeta^2 + (E_+ - G)^2 + (E_- - G)^2]} \right\}, \quad (6)$$

where  $C$  is a normalization constant,  $E$  and  $E_0$  refer to the initial state for the transition and are given by Eq. (3),  $E_{\mp}$  are given by Eq. (4), and  $k\theta$  is the zero point energy. The first factor in curly brackets gives the probability of the configuration  $q$  for the transition  $\Delta E$  and also takes account of the change in variable from  $q$  to  $\Delta E$  by means of the Jacobian  $dq/d\Delta E$ . This factor was shown in the earlier analysis<sup>6</sup> to describe the widths and temperature-dependence of these spectra. The Jacobian was found to account for the skewness of the long-wavelength absorption band. The second factor<sup>11</sup> takes account of the principal dependence of the dipole matrix element on nuclear coordinates, therefore, the model is adiabatic rather than harmonic. In applying Eq. (6) to KCl:Ti it is found that the second factor makes only a small contribution to the shape of these spectra. The harmonic analysis<sup>6</sup> is therefore confirmed as a good approximation for calculating the shape of the impurity absorption and emission bands of KCl:Ti.

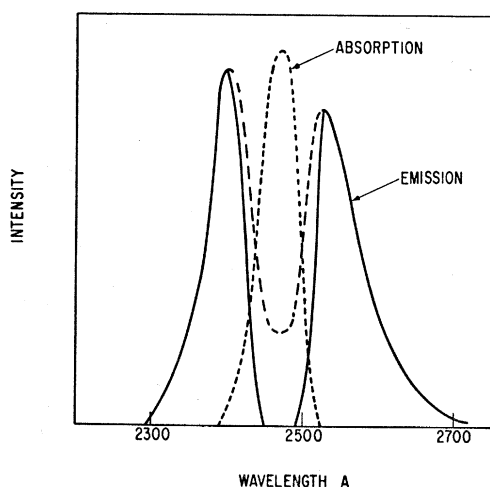


Fig. 2. Comparison of absorption and emission spectra of KCl:Ti in the 2470 Å region.

The peak positions of absorption and emission can be obtained from Fig. 1 as can the temperature dependence of the relative emission intensity of the two principal emission bands. Since the half-widths of these emission bands are strongly dependent on the exact energy contour of the lower excited state, comparison of theoretical and experimental half-widths of emission shows the correct magnitude but not quantitative agreement. The lower curve is in accord with the negligible energy barrier and with the small energy difference of 0.025 eV between the two emitting configurations which were previously deduced experimentally.<sup>8</sup> The appreciable dependence of relative emission intensity at 4750 Å and 3050 Å on activator concentration at a given temperature may be attributed to the perturbing effect of nearby, but not adjacent, activators on the relative energies of the two emitting configurations. A small shift in relative energies may affect the relative populations of the two configurations without altering the spectra of the two emission bands appreciably. The change in relative intensities of the two emission bands with temperature in any particular phosphor, along with the constant total quantum efficiency as temperature is altered, indicates approximate thermal equilibrium between the two emitting configurations. This equilibrium is disturbed only slightly by emission.<sup>8</sup>

From the value of  $2G$  at the configuration  $q_0$  of the  $^1S$  state, the oscillator strength ratio for the two impurity absorption bands is calculated to be 7, as compared to the experimental value of 5. This result differs from the calculated ratio of 2 reported earlier<sup>11</sup> because of the difference in the value of  $2G$  used in the two analyses. The peak energies in the absorption spectra differ in the two analyses by approximately 1/10 eV. This illustrates the sensitivity of the oscillator strength ratio to small changes in the transition energies.

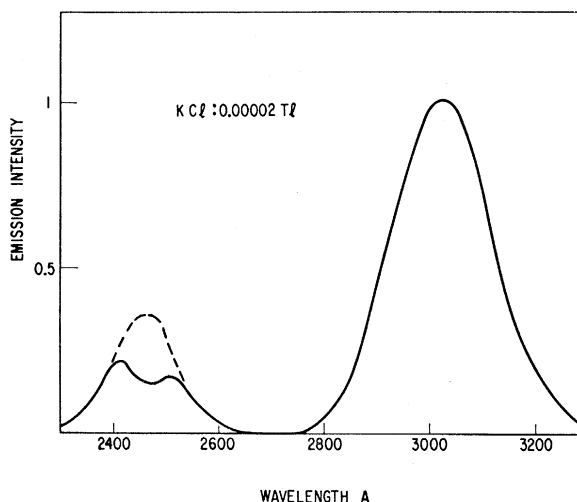


Fig. 3. Comparison of 2470 Å and 3050 Å emission bands of KCl:Ti under 1960 Å excitation.

The well-known 3050 Å and 4750 Å emission bands are accounted for by the two minima of the lower excited state. In accordance with the earlier identification<sup>8</sup> of the emitting states, the minimum responsible for the 3050 Å emission has the greater  $^3P^\circ$  character whereas the minimum responsible for the 4750 Å emission has the greater  $^1P^\circ$  character. From the present model, however, we predict an additional emission band. The transition from the single minimum of the upper excited state to the ground state should occur with appreciable probability since this state has approximately half  $^1P^\circ$  and half  $^3P^\circ$  character at the configuration of the minimum. From Fig. 1 the emission energy for this transition is found to be quite close to that of the long-wavelength absorption band. Self-absorption as well as the requirement for 1960 Å excitation could thus account for the fact that this emission band has not been reported previously.

#### IV. EXPERIMENTAL INVESTIGATION OF THE 2470 Å EMISSION

Investigation of the 2470 Å emission was undertaken using a 200-watt hydrogen lamp, in conjunction with a small  $f/4$  fused silica prism monochromator, for excitation. The monochromator was set for peak intensity at 1980 Å with 160 Å total band width. A G.E. grating spectroradiometer was used to record the emission. At room temperature no emission in the predicted range of 2200 to 2800 Å was observed. However, on immersing the crystal in liquid nitrogen, spectra such as shown in Figs. 2 and 3 for KCl:0.00002 Ti were observed. In Fig. 2 the previously determined 2470 Å absorption at this temperature<sup>12</sup> is shown for comparison. The solid curve is the emission observed when the end of the crystal away from the spectroradiometer slit is excited, and the dashed curve, when the end near the slit is excited. In both these cases the direction of excitation was perpendicular to the direction of the observed emission. The difference between these two spectra is clearly to be expected for an emission centered in the 2470 Å absorption band. In Fig. 3 the emission observed from the same side as the excitation is given as the solid line, and the dashed line is the emission after correcting for self-absorption. With excitation and emission perpendicular to the same crystal face, the emission intensity,  $I_\lambda$ , with no self-absorption at wavelength  $\lambda$  is given by the expression

$$I_\lambda = I_0(\bar{k} + k_\lambda)/\bar{k}, \quad (7)$$

where  $I_0$  is the observed emission intensity,  $k_\lambda$  is the absorption constant for emission at wavelength  $\lambda$  and

$\bar{k}$  is an average absorption constant for excitation weighted according to the spectral distribution of intensity of the excitation.

The relatively high intensity of the 3050 Å peak with 1960 Å excitation cannot be explained entirely on the basis of absorption of the 2470 Å emission. Efforts to detect infrared emission resulting from the optical transition from the upper to the lower excited state indicate that this radiative process is not the dominant mechanism for the transition. This transition is in fact forbidden because of the parity selection rule. The finite velocity of the nuclei arising from the large polarization energy following 1960 Å excitation may lead to non-adiabatic crossing to the lower excited state. Although the theory of nonadiabatic crossing of energy levels does not strictly apply to this system because of the large separation of the states and the nonuniform velocity of the nuclei, appreciable crossing to the lower state is suggested by application of the Zener formula.<sup>12</sup> An alternate mechanism for the transition could be by way of nonspherically symmetrical vibrations of the system.

In none of the crystals studied could 2470 Å emission be observed with 2537 Å excitation. Because of scattered excitation when 2470 Å radiation from the prism monochromator was used, it can be stated reliably only that the 2470 Å emission is less than 15% of its intensity, as determined by comparison with the 3050 Å band, under 1960 Å excitation. Tests with various slit widths, temperatures, and geometries for excitation lead to the conclusion that all radiation in the 2470 Å region from crystals under 2470 Å excitation is scattered excitation.

#### V. CONCLUSIONS

The effect of the crystalline field on spin-orbit interaction in the excited states of KCl:Ti has been extended throughout the range of nuclear configurations involved in the impurity absorption and emission transitions. It is possible to construct an energy-configuration coordinate diagram for this phosphor which takes into account spin-orbit interaction. This diagram is in satisfactory accord with the available spectral data, including the relative oscillator strength for the two principal impurity absorption bands. In addition, it predicts a new emission band which has now been discovered and found to have characteristics quantitatively in accord with the model.

#### VI. ACKNOWLEDGMENTS

The authors are indebted to Miss Gwen Lloyd for assistance with the spectral measurements and to Mrs. Mary Gray for much of the numerical analysis. We also acknowledge the helpful comments of Dr. B. Segall.

<sup>12</sup> C. Zener, Proc. Roy. Soc. (London) **A137**, 696 (1932); **A140**, 660 (1933).